Quality control of assembly-defective U1 snRNAs by decapping and 5′-to-3′ exonucleolytic digestion

Siddharth Shukla[a] and Roy Parker[a,b,1]

[a]Department of Chemistry and Biochemistry and [b]Howard Hughes Medical Institute, University of Colorado, Boulder, CO 80303

Contributed by Roy Parker, July 3, 2014 (sent for review June 24, 2014; reviewed by David Tollervey)

The accurate biogenesis of RNA–protein complexes is a key aspect of eukaryotic cells. Defects in Sm protein complex binding to snRNAs are known to reduce levels of snRNAs, suggesting an unknown quality control system for small nuclear ribonucleoprotein (snRNP) assembly. snRNA quality control may also be relevant in spinal muscular atrophy, which is caused by defects in the *survival motor neuron* (*SMN*)*1* gene, an assembly factor for loading the Sm complex on snRNAs and, when severely reduced, can lead to reduced levels of snRNAs and splicing defects. To determine how assembly-defective snRNAs are degraded, we first demonstrate that yeast U1 Sm-mutant snRNAs are degraded either by Rrp6- or by Dcp2-dependent decapping/5′-to-3′ decay. Knockdown of the decapping enzyme DCP2 in mammalian cells also increases the levels of assembly-defective snRNAs and suppresses some splicing defects seen in SMN-deficient cells. These results identify a conserved mechanism of snRNA quality control, and also suggest a general paradigm wherein the phenotype of an "RNP assembly disease" might be suppressed by inhibition of a competing RNA quality control mechanism.

Eukaryotic cells contain a growing diversity of functional noncoding ribonucleoprotein (RNP) complexes. The biogenesis of a stable functional RNP complex requires multiple RNA-processing reactions and assembly with specific RNA-binding proteins. To prevent the formation of aberrant RNPs and to increase the specificity of RNP assembly, eukaryotic cells also contain a number of RNA quality control systems that recognize and degrade aberrant RNAs (1, 2). The full spectrum of RNA quality control mechanisms and their biological impacts remains to be determined.

snRNAs may be subject to quality control mechanisms, because mutations in the binding site for the Sm protein complex reduce steady-state snRNA levels, although whether this is directly due to specific RNA decay mechanisms has not been explored (3–5). snRNA quality control may also be triggered by defects in assembly factors. For example, spinal muscular atrophy (SMA) is a neurodegenerative disease caused by low levels of the survival motor neuron (SMN) protein due to mutations in the principal SMN-coding gene *SMN1* (6, 7). One role of the SMN complex is to load the Sm protein complex onto the Sm site on snRNAs, which has a consensus sequence of $PuAU_{4-6}GPu$ (8–10). Animal models of SMA, as well as in vitro analysis of SMN knockdown cell lines, revealed that a severe decrease in SMN levels leads to a nonuniform reduction in the levels of snRNAs and snRNPs, further leading to perturbations in splicing (11–16). There are contrasting views as to whether the snRNP assembly function of SMN is causative of SMA (17). Transcriptome analysis in some SMN mutant animal models reveals few splicing defects early in disease progression and, at least in *Drosophila*, raises the possibility that toxicity could be due to SMN deficiency triggering a stress response (18–20). At the same time, expression of mature snRNPs can rescue motor function deficit in another SMA model (21), and splicing defects have been identified in genes that are important for proper development and function of motor neurons from other disease models (14, 16, 22). One way to address the role of snRNA degradation in SMA is to identify the mechanisms by which assembly-defective snRNAs are degraded and then examine how disruption of such snRNA decay mechanisms affects SMN mutant phenotypes.

Herein we use yeast and mammalian cells to identify snRNA quality control systems that degrade snRNAs when Sm complex assembly is limiting. In yeast, snRNAs defective in Sm complex assembly are subject to quality control both by 3′-to-5′ decay in the nucleus and by decapping and 5′-to-3′ cytoplasmic decay. Strikingly, decapping and 5′-to-3′ degradation is conserved for mammalian snRNAs defective in Sm complex assembly, either due to mutations in the Sm site or to reduced levels of the SMN complex. Moreover, splicing defects seen in SMN-deficient cells can be partially suppressed by knockdown of the DCP2 decapping enzyme. These results identify specific snRNA quality control mechanisms in eukaryotic cells. This work also raises the possibility of a general paradigm wherein the effect of mutations that cause disease by limiting RNP assembly, referred to as "RNP assembly diseases," might, at least in some cases, be ameliorated by inhibition of the competing RNA quality control mechanism.

Results

Mutations in the Yeast U1 snRNA Sm Site Destabilize snRNA. To identify quality control mechanisms for snRNAs, we first analyzed the decay of yeast U1 snRNAs defective in binding the Sm complex. We expressed exogenous U1 snRNA from a galactose-regulated promoter, which allows repression of transcription with glucose to measure RNA decay rates. To specifically detect exogenous U1 snRNA, it included the HVII-m2 mutations, which are neutral base changes in helical loop VII (23). To mimic defects in loading of the Sm complex caused by reduced levels of the SMN protein in SMA, we created two different mutations in the yeast U1 Sm site (AUUUUUG; Fig. 1*A*). The first Sm mutant, hereafter referred to as U1-C2, has the mutated

Significance

Cellular RNAs undergo assembly with various proteins, which leads to the formation of functional ribonucleoprotein (RNP) complexes. Kinetic defects in the RNP assembly pathway, which affect the rate of RNP formation, can lead to a reduction in the levels of functional RNPs in the cell, and can lead to a disease state, which we classify as an "RNP assembly disease." One example of this class of diseases is spinal muscular atrophy (SMA), where mutations in the assembly factor survival motor neuron lead to reduced small nuclear (sn)RNA and snRNP levels. Here we describe the decay pathways that regulate snRNA levels and function in the cell, prevention of which could be pertinent as a therapy for SMA.

Author contributions: S.S. and R.P. designed research; S.S. performed research; S.S. and R.P. analyzed data; and S.S. and R.P. wrote the paper.

Reviewers included: D.T., University of Edinburgh.

The authors declare no conflict of interest.

Freely available online through the PNAS open access option.

[1]To whom correspondence should be addressed. Email: roy.parker@colorado.edu.

This article contains supporting information online at www.pnas.org/lookup/suppl/doi:10.1073/pnas.1412614111/-/DCSupplemental.

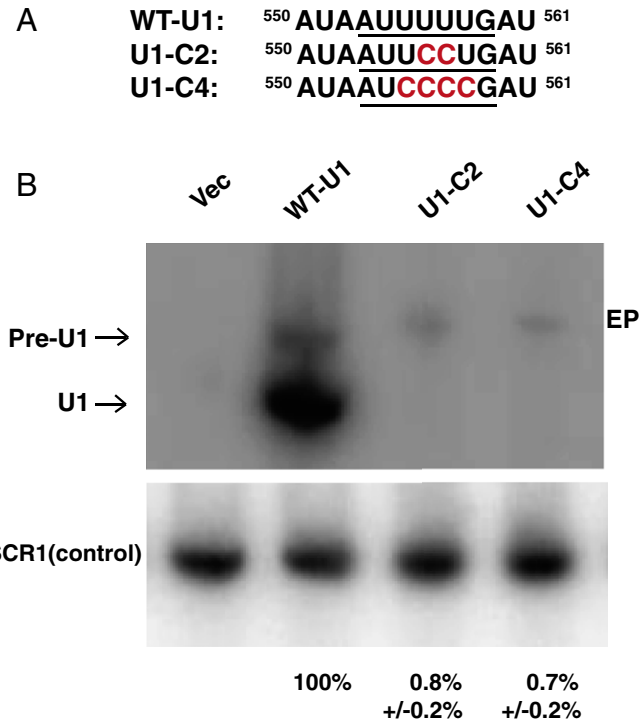

Fig. 1. Yeast U1 Sm-mutant RNAs are unstable and rapidly degraded by quality control mechanisms. (*A*) The 3′ end sequence starting from base 550 for the 568 bases-long *Saccharomyces cerevisiae* U1 snRNA is shown. The wild-type Sm sequence is underlined (mutations are in red). (*B*) Representative steady-state Northern image depicting the levels of the wild-type and Sm-mutant U1 snRNA in a yRP840 strain. The probe is an oligonucleotide specific for the Gal-expressed exogenous U1 RNA. EP, extended precursor species. Quantification of four independent experiments with averages and SDs is shown below each lane.

sequence AUUCCUG, whereas the second Sm mutant, hereafter referred to as U1-C4, has the mutated sequence AUCCCCG.

Expression of the U1-C2 and U1-C4 mutants in a wild-type background in yeast revealed that both mutations reduced the levels of U1 snRNAs to <1% of the comparable wild-type U1 snRNA (Fig. 1*B*). We also observed that the residual U1-C2 and U1-C4 snRNAs detected were longer than the mature wild-type U1 (Fig. 1*B*). This is consistent with earlier results that mutations in the Sm site of U1 snRNA alter its 3′ processing, leading to species that are ∼75 nt longer than the WT 3′ end of U1 snRNA (24).

This reduction of U1-C2 and U1-C4 snRNA levels could be due to decreased transcription or increased decay. However, by blocking transcription with glucose and following snRNA levels over time, we observed that the low steady-state level of U1-C2 and U1-C4 snRNAs is due to their rapid degradation (Fig. 2*A*). In comparison, WT-U1 snRNA is highly stable after inhibition of transcription. These observations indicate that defects in the Sm binding site of U1 snRNAs lead to their rapid degradation.

Defective U1 snRNAs Are Degraded by Both 3′-to-5′ Exonuclease Rrp6 and Decapping and Xrn1-Mediated Decay. To identify the nucleolytic pathways that degrade the U1-C2 and U1-C4 mutant snRNAs, we introduced their expression plasmids into a number of yeast strains lacking components of different nuclear and cytoplasmic RNA degradation pathways (Table S1) (25) and examined their steady-state levels in log phase of growth.

An important observation was that U1-C2 and U1-C4 mutant snRNA levels were significantly higher in the *rrp6Δ*, *trf4Δ*, *xrn1Δ*, and *dcp1Δ* strains compared with wild type (Fig. 2 *B* and *C*). In contrast, the U1-C2 and U1-C4 snRNA levels did not significantly increase in the *rai1*Δ, *ski7*Δ, and *edc3*Δ strains. These effects were specific to the U1-C2 and U1-C4 RNAs, because the steady-state level of the wild-type U1 snRNA was not altered in any of the RNA decay mutants (Fig. S1*A*). The effect of Rrp6, which is a nuclear 3′-to-5′ exonuclease (26), and Trf4, which is a nuclear poly(A) polymerase that adenylates RNAs to promote their 3′-to-5′ degradation (27–30), suggests that U1-C2 and U1-C4 snRNAs can be degraded by a 3′-to-5′ nuclear decay mechanism. In addition, the effect of *dcp1*Δ and *xrn1*Δ on the levels of U1-C2 and U1-C4 RNAs suggests that these mutant snRNAs can also be degraded by decapping and 5′-to-3′ digestion.

To determine whether the increase in the mutant snRNA steady-state levels seen in these mutant strains was due to an effect on their rate of degradation, we measured the decay rates of U1-C2 and U1-C4 snRNAs in the *trf4*Δ, *rrp6*Δ, *dcp1*Δ, and *xrn1*Δ strains. We observed that *xrn1*Δ, *rrp6*Δ, *trf4*Δ, and *dcp1*Δ all increased the stability of both the U1-C2 and U1-C4 snRNAs (Fig. 2 *D* and *E*). In contrast, the decay rates of U1-C2 and U1-C4 snRNAs are not affected by inhibition of cytoplasmic 3′-to-5′ degradation dependent on the Ski complex (Fig. 2*D*). We interpret the altered decay rates in the *xrn1*Δ, *dcp1*Δ, *trf4*Δ, and *rrp6*Δ strains to indicate that U1-C2 and U1-C4 snRNAs can be degraded by adenylation and 3′-to-5′ decay in the nucleus, as well as by a second pathway consisting of decapping and 5′-to-3′ decay, which is most likely cytoplasmic.

In the simplest model, the 3′-to-5′ and decapping/5′-to-3′ decay pathways for the mutant U1 snRNAs would be independent and function redundantly to limit the production of aberrant snRNAs. This model predicts that strains defective in both pathways should show an additive or synergistic increase in the levels and stability of the mutant snRNAs. To test this prediction, we examined the steady-state levels of the wild-type and mutant snRNAs in an *xrn1*Δ *rrp6*Δ double mutant. Strikingly, we observed that by inhibiting both decay pathways, the levels and stability of the mutant snRNAs were restored almost to wild-type U1 snRNA levels [compare mutant snRNA levels between the wild type (∼1% of WT-U1) and *xrn1*Δ *rrp6*Δ strain] (Fig. 3 *A* and *B*). These observations demonstrate that the U1-C2 and U1-C4 snRNAs are degraded by two independent and redundant decay mechanisms, and that inactivation of both pathways strongly increases the levels and stability of the mutant snRNAs (Fig. 3*C*).

Another interesting observation was that the level and stability of the wild-type U1 precursor was increased in the *xrn1*Δ *rrp6*Δ strain (Fig. 3*B* and Fig. S1*B*). This suggests that the Gal promoter-driven U1 RNA is being produced in excess and U1 RNA molecules that are unable to be assembled into snRNPs are degraded by these two decay mechanisms. Consistent with this view, we observe that whereas the decay rate of wild-type mature U1 snRNA is not affected by *xrn1*Δ *rrp6*Δ, the pre-U1 snRNA is stabilized (Fig. S1*B*). This indicates that quality control mechanisms for snRNAs may not only play a role in degrading snRNAs defective in assembly reactions but can also function to maintain the proper level of snRNA relative to the protein components of the snRNP.

Decapping of Defective U1 snRNAs in Yeast Is Catalyzed by the Dcp2 Enzyme. In principle, the smaller effects of *dcp1*Δ on the decay rate of U1-C2 and U1-C4 snRNAs could be due to the involvement of multiple decapping enzymes in their degradation. Specifically, work has identified the Dcs1, Rai1, and Dxo1 proteins as additional yeast decapping enzymes (31–33). In our initial screen of yeast mutations affecting RNA decay, we did not see any effect of *rai1*Δ on U1-C2 or U1-C4 snRNAs (Fig. 2 *B* and *C*). To test whether another decapping enzyme could be involved in U1-C2 and U1-C4 snRNA decay, we examined the steady-state levels in a mutant strain lacking Dcs1, which is a cytoplasmic scavenger decapping enzyme that can remove the m^7G cap, or a strain lacking Dcp2, which is the catalytic subunit of the major mRNA decapping enzyme complex that works with Dcp1.

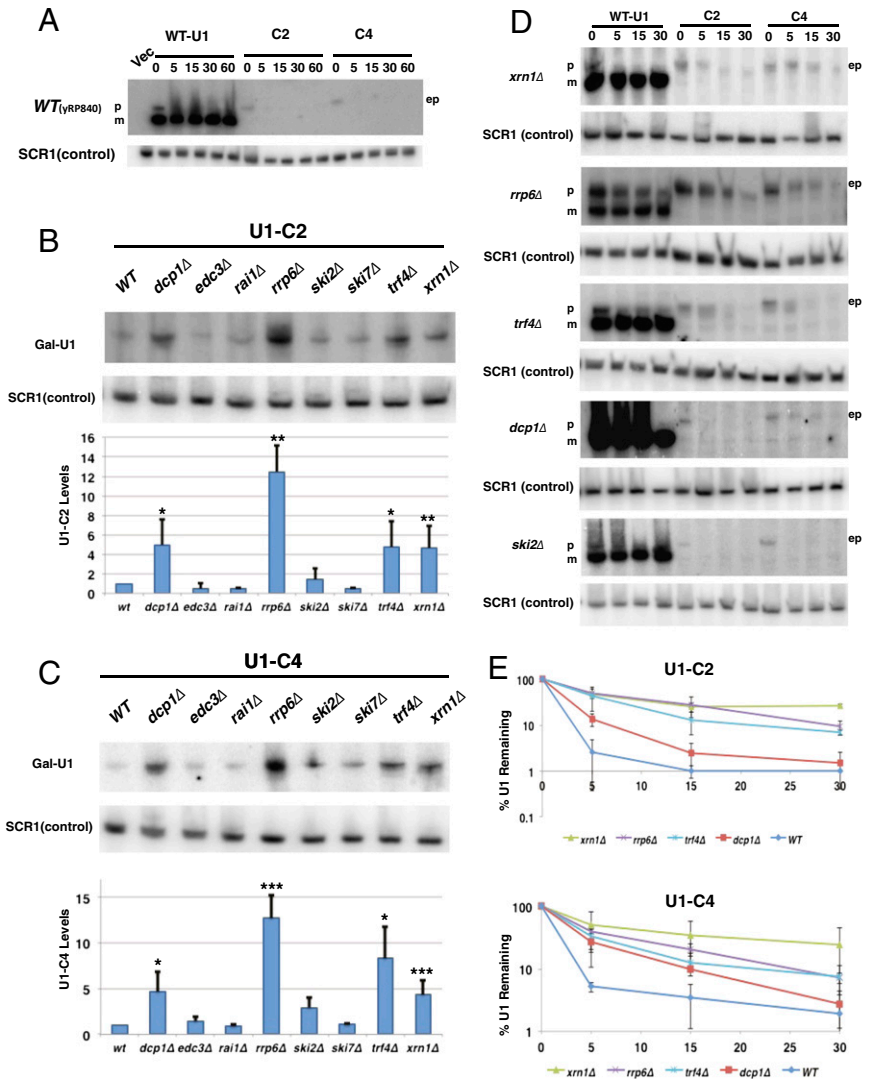

Fig. 2. Mutant U1 snRNA levels vary in various deletion strains specific to quality control in the nucleus and cytoplasm. (*A*) Representative Northern image for a time course experiment for WT-U1 and Sm-mutant RNA in a wild-type strain. ep, extended precursor species; m and p, mature and precursor WT-U1 species, respectively. (*B* and *C*) Representative Northern image depicting (*B*) steady-state U1-C2 RNA levels and (*C*) steady-state U1-C4 RNA levels in various deletion strains. A histogram depicting averages and SDs, along with significant differences (*$P < 0.05$, **$P < 0.01$, ***$P < 0.001$) between the snRNA levels in various deletion strains compared with the *WT* strain for at least three independent replicates, is also depicted. *P* values were calculated using one-tailed unpaired Student's *t* test. (*D*) Representative Northern images depicting the time course experiment for WT-U1, U1-C2, and U1-C4 snRNAs in various deletion strains. (*E*) Quantification of three independent time course experiments in various deletions strains as labeled. The semilogarithmic plot depicts the average RNA levels (±SD) as a percentage of 0 min on the *y* axis.

We also examined the U1-C2 and U1-C4 snRNA levels in a *dxo1Δ* strain, which lacks the Dxo1 enzyme believed to specifically remove unmethylated defective mRNA caps (32).

We observed that *dcs1*Δ or *dcp2Δ* did not significantly increase the U1-C2 or U1-C4 snRNA levels (Fig. 3*D*). We also did not see any measurable difference in the snRNA levels between the *WT* and *dxo1Δ* strains, consistent with its specificity for unmethylated caps (32). Surprisingly, we observed a small but consistent decrease in the steady-state levels of these snRNAs in the *dcp2*Δ strain, which may be explained by a decrease in global transcription in *dcp2*Δ strains (34). This complicating effect of *dcp2*Δ mutants on transcription suggested that we needed to directly measure the snRNA decay rate in strains defective in Dcp2's activity to establish whether Dcp2 is involved in the decapping of snRNAs before their 5′-to-3′ digestion by Xrn1.

To do this experiment, we took advantage of the synergistic effect of *xrn1*Δ with *rrp6*Δ on U1-C2 and U1-C4 degradation, which suggested that we could also examine the effect of decapping defects on U1-C2 and U1-C4 snRNA decay by making double mutants with *rrp6*Δ. This experiment has the advantage of testing the effect of decapping mutations when the alternative 3′-to-5′ degradation pathway is inhibited, and therefore any effect will have a larger consequence on snRNA decay. Thus, we created *dcs1*Δ *rrp6*Δ and *dcp2-7 rrp6*Δ strains and used these strains to directly measure the effects of *dcp2-7* and *dcs1*Δ mutations on snRNA decay. The *dcp2-7* strain is a temperature-sensitive allele of Dcp2 (35), which we used because a *dcp2*Δ *rrp6*Δ strain was synthetically lethal (data not shown).

We observed that the *dcp2-7 rrp6*Δ strain showed a slow decay rate of the defective snRNAs after a shift to restrictive temperature (Fig. 3*E*), suggesting that the Dcp1/Dcp2 enzyme is responsible for snRNA decapping. In contrast, the *dcs1*Δ *rrp6*Δ strain behaved similar to *rrp6*Δ (Fig. 3*F*). We interpret these observations to indicate that the major decapping enzyme for

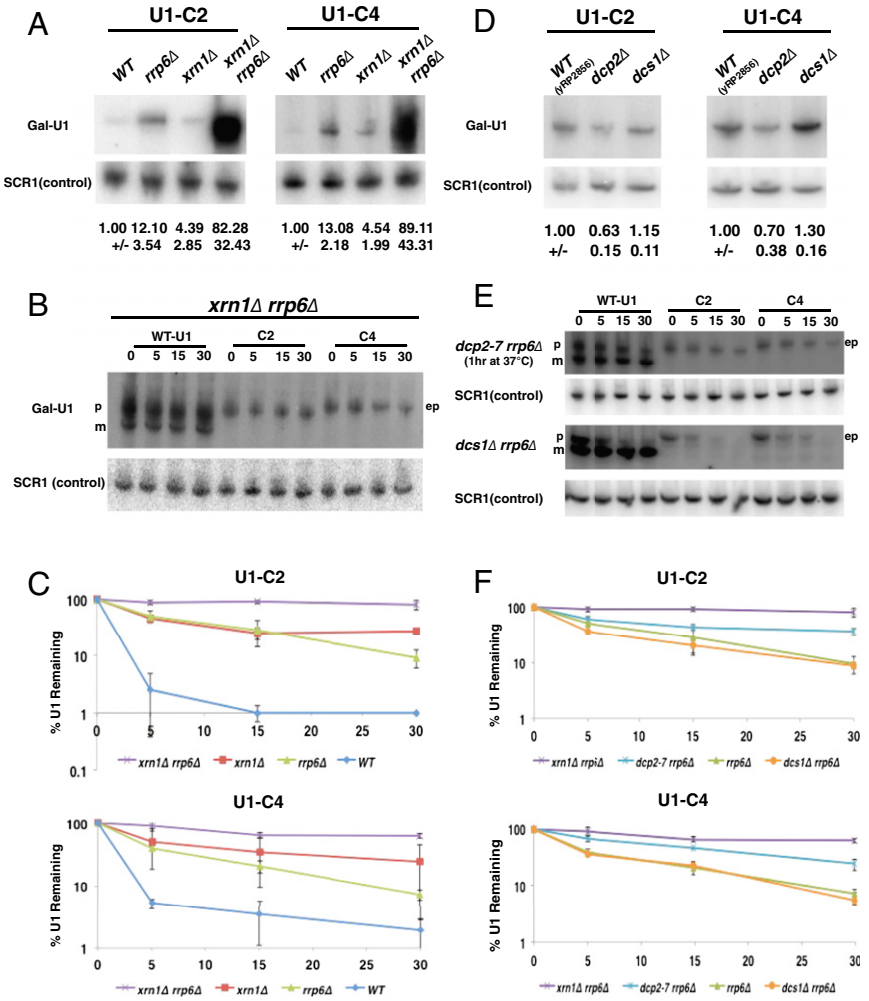

Fig. 3. Two independent yeast snRNA quality control mechanisms. (*A*) Representative Northern image depicting the steady-state levels of U1-C2 and U1-C4 snRNA levels in the indicated deletion strains. Quantification of four independent experiments with averages and SDs is shown below each lane. (*B*) Representative Northern image of the time course experiment for WT-U1, U1-C2, and U1-C4 snRNAs in the *xrn1Δ rrp6Δ* strain. (*C*) Quantification of three independent RNA decay rate experiments in the *xrn1Δ rrp6Δ* strain as a percentage of 0 min (average ± SD). (*D*) Representative Northern image depicting steady-state RNA levels along with quantification of four independent replicates (average ± SD) below each lane for various decapping mutants. (*E*) Representative Northern images for the time course experiment for WT-U1, U1-C2, and U1-C4 snRNAs in the *dcp2-7 rrp6Δ* and *dcs1Δ rrp6Δ* strains, respectively. (*F*) Quantification of three independent time course experiments in various strains, as indicated. The semilogarithmic plot depicts RNA levels as a percentage of 0 min on the *y* axis (average ± SD).

defective snRNAs is the Dcp1/Dcp2 holoenzyme, which is consistent with the increase in mutant snRNA levels in the *dcp1Δ* strain.

Taken together, these results argue that yeast snRNAs defective in Sm complex assembly are degraded independently by 3′-to-5′ and decapping/5′-to-3′ decay mechanisms. Because Sm complex association with snRNAs in yeast has been proposed to occur in the nucleus (3), we suggest that Sm assembly on yeast snRNAs first competes with nuclear 3′-to-5′ degradation by Rrp6. However, given that yeast snRNAs can enter the cytosol (36) and Dcp2/Xrn1 activity is primarily cytoplasmic (25), we speculate that nuclear 3′-to-5′ decay also competes with snRNA export to the cytosol, and that exported snRNAs are subject to subsequent decapping by Dcp1/Dcp2 and 5′-to-3′ degradation by Xrn1.

Decapping and 5′-to-3′ Degradation of Defective snRNAs Is Conserved in Mammalian Cells. To determine whether these snRNA quality control pathways are conserved in humans, we first created human U1 snRNA plasmids that contain analogous C2 and C4 mutations in their Sm site. These U1 gene plasmids also have additional mutations in the stem loop III region, which do not disrupt the function of the U1 snRNA but allow for specific detection of exogenous U1 RNA (37).

We measured the levels of U1-C2 (human) and U1-C4 (human) snRNAs in HeLa cells after transient transfection of the respective plasmids for 24 h. We found that the U1-C2 and U1-C4 RNA levels are ∼15% and 10% of the WT-U1 RNA in the cell, respectively (Fig. 4*A*). We interpret the reduced levels of the U1-C2 and U1-C4 snRNAs to indicate that these defective snRNAs are degraded more rapidly than wild-type U1 snRNA.

To determine whether the role of RRP6 and XRN1 was conserved in human snRNA quality control, we used siRNA knockdown of these components (Fig. 4*B*) and examined the levels of U1-C4 (human) snRNA after transient transfection. We found that the knockdown of the XRN1 enzyme increased the levels of U1-C4 snRNA, whereas knockdown of EXOSC10 (mammalian ortholog of Rrp6) does not have an effect on U1-C4 snRNA levels (Fig. 4 *C* and *D*). This suggests that the decapping and 5′-to-3′ decay of snRNAs is conserved in mammalian cells, whereas the role for RRP6 in snRNA quality control is not. Although we cannot rule out the formal possibility

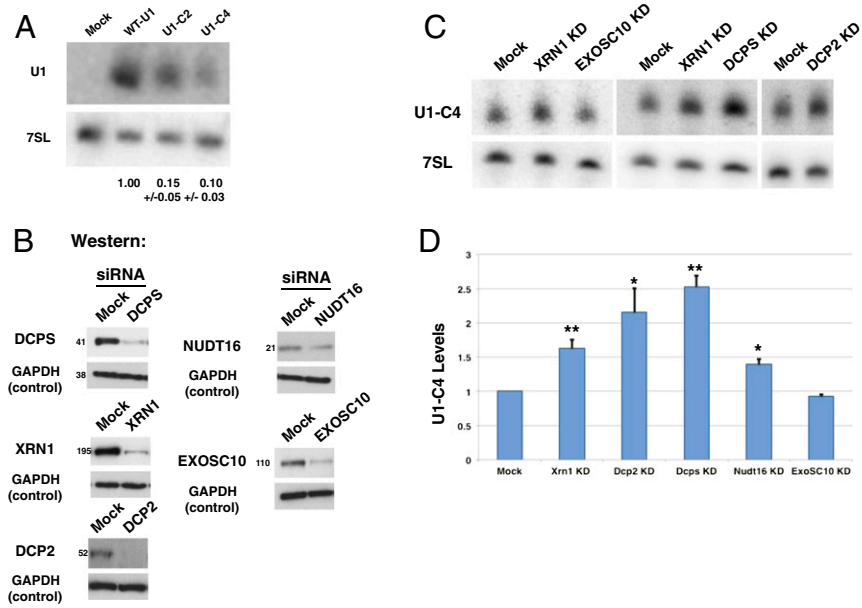

Fig. 4. Mammalian snRNAs with defects in the Sm site are degraded by XRN1. (*A*) Representative Northern image depicting WT-U1 or Sm-mutant snRNA levels in HeLa cells. Quantification of three independent experiments with averages and SDs is depicted below each lane. (*B*) Representative Western blot images for knockdowns of various targets during the U1 plasmid cotransfection experiment. GAPDH was used as a loading control. The predicted molecular weight corresponding to each band is also indicated. (*C*) Representative Northern images for U1-C4 RNA under various knockdown conditions compared with mock knockdown. 7SL RNA was used as a loading control. (*D*) Histogram depicting the average steady-state U1-C4 RNA levels along with SDs in various knockdown conditions, as indicated. Significant differences (*$P < 0.05$, **$P < 0.01$) from the mock transfection group for at least three independent replicates are shown. *P* values were calculated for each group using one-tailed unpaired Student's *t* test.

that EXOSC10 is involved, RNAi knockdown was not sufficient to reveal a phenotype. The greater importance of cytoplasmic decay mechanisms in mammalian cells could be because snRNAs are exported from the nucleus and assembled with the Sm complex in the cytosol in mammals (10), and therefore defects in Sm assembly would be expected to primarily expose the snRNAs to cytoplasmic decay mechanisms.

Mammalian cells contain a greater diversity of decapping enzymes than yeast (38–40). To determine whether one or more decapping enzymes were involved in snRNA quality control, we examined siRNA knockdown of human DCP2, DCPS (the human ortholog of Dcs1), and NUDT16, a decapping enzyme that can work on small nucleolar RNAs and some mRNAs (38, 41), along with transient transfection of U1-C4 snRNA in HeLa cells. We observed that knockdown of DCPS led to a 2.5-fold increase in U1-C4 (human) RNA levels in the cell and DCP2 knockdown gave a 2-fold increase, whereas NUDT16 had only an ∼1.3-fold increase (Fig. 4*D* and Fig. S2). This suggests that DCPS and DCP2 can affect snRNA quality control in humans (*Discussion*).

Reduction of snRNA Levels by SMN Knockdown Can Be Rescued by Inhibition of Decapping and XRN1-Mediated Decay. In spinal muscular atrophy, the levels of snRNAs are reduced due to mutations limiting the levels of the SMN protein, which is an assembly factor for the loading of Sm complex on snRNAs (11, 42–44). Because limiting Sm complex loading on snRNA by defects in the SMN complex is analogous to limiting it by mutations in the Sm site, we predicted that the reductions in snRNA levels when SMN is defective should be rescued by inhibition of cytoplasmic decapping and the 5′-to-3′ degradation pathway. To test this prediction, we examined the levels of various snRNAs in response to SMN knockdown, with or without knockdown of decapping enzymes or XRN1 (Fig. S3 *A* and *B*). Consistent with earlier results (12, 14, 15, 19), we observed that SMN knockdown reduced levels of U1, U5, U11, U12, and U4atac snRNAs (Fig. 5 *A* and *B*). We did not examine U2 and U4 snRNAs because they were previously shown to be the least susceptible to SMN KD in cell-culture experiments (12, 14).

We observed that knockdown of XRN1 in addition to SMN knockdown restored the levels of these snRNAs to their native levels (Fig. 5 *C* and *D*). In contrast, we saw no significant effect on snRNA levels in an SMN and EXOSC10 double-knockdown experiment. This is consistent with our results for U1-C4 (human) mutant snRNA and argues that inefficient Sm assembly leads to cytoplasmic 5′-to-3′ decay.

Examination of the various mammalian decapping enzymes suggests that knockdown of DCP2 and/or DCPS can partially restore the levels of U1, U5, U11, U12, and U4atac that are reduced due to SMN knockdown (Fig. 5*D*), suggesting these enzymes play a role in the degradation of snRNAs in mammalian cells (*Discussion*). These results argue that decapping and XRN1-mediated degradation compete with SMN-mediated assembly of the Sm complex on snRNAs and, when SMN levels are reduced, the degradation of snRNAs outcompetes assembly with the Sm complex.

Knockdown of DCP2 Partially Suppresses Some SMN Knockdown-Dependent Splicing Defects. We next investigated whether the rescue of snRNA levels by knockdown of the components of the cytoplasmic 5′-to-3′ decay pathway is functionally relevant in rescuing the splicing defects previously observed in SMN mutant models (12, 14). To address this question, we used the NIH 3T3 mouse fibroblast cell line wherein splicing defects due to SMN knockdown in U12-dependent introns have been identified (14). We first reproduced earlier results wherein SMN knockdown results in altered splicing as assessed by the accumulation of precursor at the expense of mature mRNA for C19orf54, Vps16, and Parp1 mRNAs (Fig. 6*A* and Figs. S4 *A* and *B* and S5*A*). We then examined whether this defect in splicing due to SMN knockdown could be affected by additional knockdowns of DCP2 or XRN1.

An important result was that DCP2 knockdown, but not XRN1 knockdown, partially suppressed the splicing defect observed in

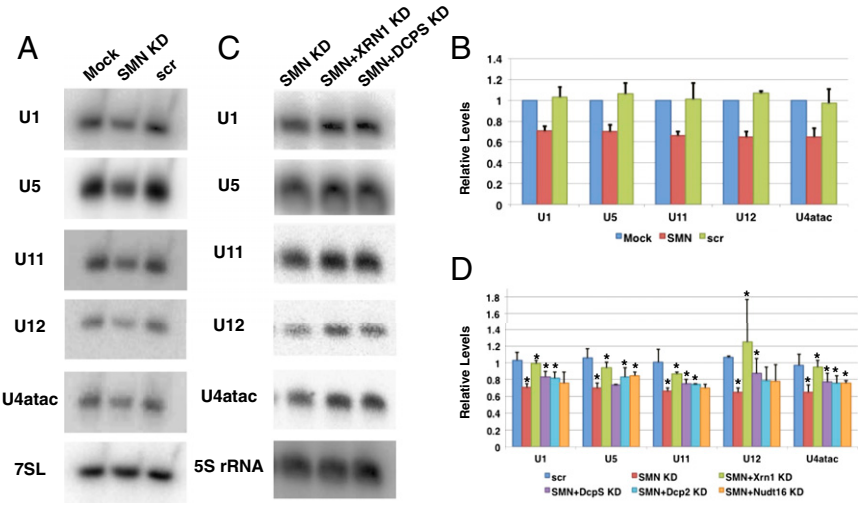

Fig. 5. Reduced snRNA levels in SMN-limiting conditions are increased by XRN1 knockdown. (*A*) Representative Northern blot for snRNA levels in HeLa cells under various transfection conditions. 7SL RNA was used as a loading control. (*B*) Quantification of four independent replicates for snRNA levels in SMN KD cells compared with control transfected cells (average ± SD). (*C*) Representative Northern blot showing snRNA levels in HeLa cells under various transfection conditions. Cells were transfected with 25 nM SMN siRNA on day 1, followed by transfection with the second siRNA (25 nM) targeting a gene of interest on day 2. Coknockdown of XRN1 and SMN restores snRNA levels to their native levels, whereas DCPS knockdown has a lesser effect. 5S rRNA was used as a loading control. (*D*) Histogram depicting average snRNA levels with SD under various transfection conditions. Significant differences were calculated using one-way ANOVA for all groups, and subsequently *P* values were calculated for each group individually using one-tailed unpaired Student's *t* test. Above red bar: $*P < 0.05$ for SMN KD alone compared with control. Above other bars: $*P < 0.05$ for double knockdowns compared with SMN KD alone.

the SMN knockdown cells, as seen by an increase in the (mature:precursor) ratio for the C19orf54 and Vps16 transcripts. (Fig. 6*A*). We also saw a small but reproducible effect of DCP2 knockdown on the Parp1 mRNA splicing defect in SMN knockdown cells (Fig. S5*A*). Importantly, for each mRNA, DCP2 knockdown alone in the absence of SMN knockdown does not significantly affect the ratio of mature:precursor transcript for either of the tested mRNAs, indicating that the effect of DCP2 knockdown is only seen when SMN is limiting (compare Scr and DCP2 KD lanes in Fig. 6*A* and Fig. S5*A*). We also observed a significant but small effect of DCPS knockdown on the splicing of C19orf54 mRNA in SMN knockdown cells ($P = 0.03$) (Fig. S5*B*). This suggests that the DCPS enzyme has a secondary role in snRNA quality control compared with the DCP2 enzyme (*Discussion*).

We next investigated whether the effect of DCP2 or XRN1 knockdown on splicing defects in SMN KD NIH 3T3 cells correlates with changes in the levels of U11 and U12 snRNAs under these transfection conditions. Similar to our results with HeLa cells, we observed that SMN knockdown gave an ∼35% decrease in the levels of U11 and U12 snRNAs, which could be partially restored by DCP2 or XRN1 knockdown (Fig. 6 *B* and *C* and Fig. S4 *A* and *B*). We interpret these results to suggest that prevention of decapping by DCP2 knockdown leads to a slight increase in snRNA levels, and this increase is sufficient to partially rescue the splicing defects observed for C19orf54 mRNA. We suggest that the failure of XRN1 knockdown to suppress the splicing defect, despite having a similar effect on snRNA levels, is because inhibition of XRN1 would be expected to lead to the accumulation of uncapped snRNAs, which presumably would be nonfunctional.

Discussion

Assembly-Defective snRNAs Are Subject to Quality Control. We present several lines of evidence that defects in snRNP assembly cause snRNAs to be cleared from cells by specific RNA quality control mechanisms. First, yeast U1 snRNAs with mutations in the Sm binding site show reduced steady-state levels and faster RNA decay rates (Fig. 1). Second, similar mutations in the Sm site of human U1 snRNA reduce its steady-state level (Fig. 4). Third, knockdown of the Sm complex assembly factor SMN leads to reduced snRNA levels in human cells (Figs. 5 and 6), which is consistent with earlier work (11–14). Finally, mutations in specific RNA nucleases increase the stability and/or steady-state levels of the defective snRNAs (Figs. 2–6). These observations demonstrate that assembly-defective snRNAs are subject to accelerated RNA degradation.

Yeast snRNAs Are Subject to Two Quality Control Mechanisms. We show that defective U1 snRNAs in yeast are degraded via two independent RNA quality control pathways: a nuclear pathway requiring Trf4 and Rrp6, and Dcp1/Dcp2-mediated decapping followed by degradation by Xrn1. Evidence for these pathways degrading defective snRNAs includes that the steady-state levels of the U1-C2 and U1-C4 RNAs increase in the *rrp6Δ*, *trf4Δ*, *xrn1Δ*, and *dcp1Δ* strains (Fig. 2 *B* and *C*). Moreover, the increase in steady-state levels of these RNAs is correlated with an increase in RNA stability in these strains (Figs. 2 *D* and *E* and 3*E*). Finally, inhibition of both of these decay pathways in the *xrn1Δ rrp6Δ* or *dcp2-7 rrp6*Δ strains leads to a synergistic increase in the steady-state levels in *xrn1Δ rrp6Δ* as well as an increase in the stability of U1-C2 and U1-C4 RNAs (Fig. 3). We interpret these results to suggest that in the nucleus, Sm complex binding competes with both Rrp6-mediated decay and export to the cytoplasm, where defective snRNAs are also subject to decapping and 5′-to-3′ decay (Fig. 7*A*), although we cannot rule out the formal possibility that Dcp2 and Xrn1 could be degrading snRNAs in the nucleus.

Defects in snRNP Assembly in Mammals Lead to Decapping and 5′-to-3′ Decay. Several lines of evidence indicate that mammalian snRNAs with defects in snRNP assembly are unstable and are subject to accelerated decapping followed by decay in a 5′-to-3′ direction by XRN1 (Fig. 7*B*). First, the reduction in human U1 snRNA levels due to mutations in the Sm site can be at least partially restored by knockdown of decapping enzymes or Xrn1 (Fig. 4). Second, the reduction in snRNA levels seen when SMN is limiting can also at least partially be restored by knockdown of XRN1 or

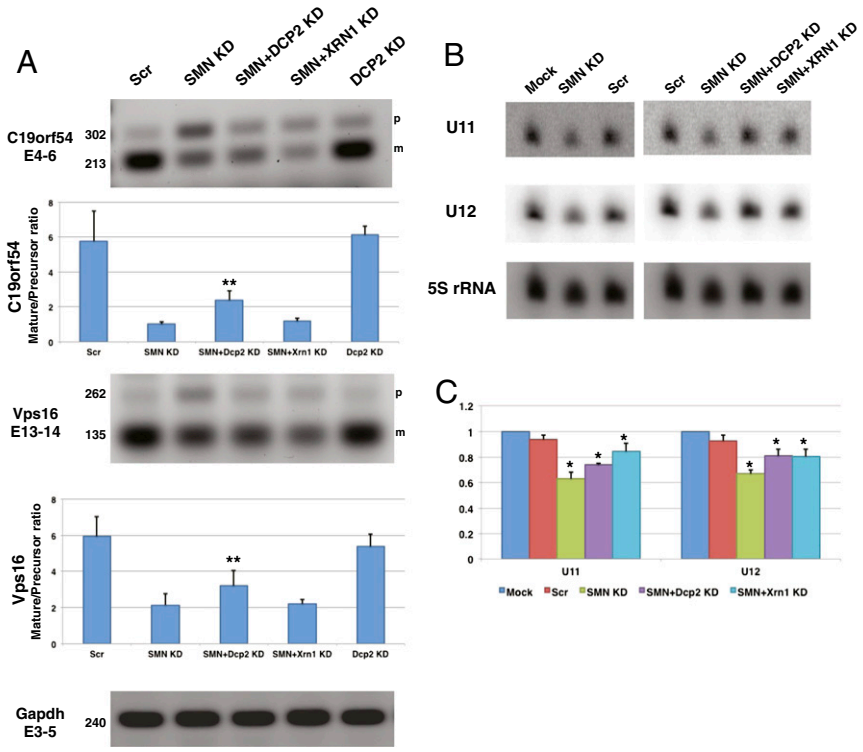

Fig. 6. DCP2 KD leads to rescue of splicing defects observed upon SMN depletion. (*A*) (*Upper*) Representative image for the PCR amplification of the indicated region of C19orf54 or Vps16 mRNA under different transfection conditions. m and p, mature and precursor transcript product, respectively. GAPDH mRNA was used as an internal loading control. (*Lower*) Quantification of at least four independent replicates (average ± SD) for each mRNA. Significant differences in the double knockdown from SMN KD alone were calculated using one-tailed unpaired Student's *t* test (**$P < 0.01$). (*B*) Representative Northern images depicting U11 and U12 snRNA levels under various knockdown conditions. 5S rRNA was used as a loading control. (*C*) Quantification of three independent replicates (average ± SD) for snRNA levels in NIH 3T3 cells. Significant differences were calculated using one-way ANOVA, followed by subsequent one-tailed unpaired Student's *t* test to identify individual *P* values. Above green bar: *$P < 0.05$ for SMN KD alone compared with control. Above other bars: *$P < 0.05$ for the double knockdowns compared with SMN KD alone.

decapping enzymes (Figs. 5 and 6). A role for decapping in mammalian snRNA decay is consistent with truncated U1 snRNAs accumulating in P bodies (45), where the decapping machinery is concentrated (46, 47). In contrast, despite efficient knockdown of the mammalian RRP6 (EXOSC10), we did not observe any effect on the levels of human mutant U1 snRNAs (Fig. 4), which argues that RRP6-mediated decay of mammalian snRNAs in response to defects in Sm loading is minimal. A predominant role for cytoplasmic decapping and 5′-to-3′ decay for mammalian snRNP quality control is appropriate because loading of the Sm complex on snRNAs is cytoplasmic followed by reimport of the snRNP to the nucleus (8).

Our results suggest that multiple decapping enzymes can affect mammalian snRNA quality control. First, knockdown of DCPS and DCP2 increased the levels of U1 Sm-mutant RNA (Fig. 4 and Fig. S2). Second, snRNA levels in SMN knockdown cells can be restored to some extent by DCPS or DCP2 knockdown (Figs. 5 and 6*C*). The effect of multiple decapping enzymes on snRNAs can be explained by direct effects of redundant decapping enzymes in mammals (38–40, 48, 49). Alternatively, the effects of some decapping enzymes could be indirect, in that knockdown of one decapping enzyme could titrate the other enzyme away from its normal RNA target, leading to stabilization of those transcripts that would otherwise be decapped specifically by these enzymes. Finally, it is possible that DCP2 is the primary enzyme for decapping of snRNA substrates in mammals, whereas the main role of DCPS, and hence its effect on snRNA levels, is through its ability to directly stimulate XRN1's activity (50, 51). This latter possibility is supported by observations that DCPS can affect XRN1-mediated microRNA decay through its interaction with XRN1 and independent of its decapping activity (52). Consistent with DCPS affecting snRNAs through XRN1 stimulation, DCPS and XRN1 knockdown both give increased snRNA levels with none or limited effects on the splicing defects in the SMN knockdown, which is in contrast to DCP2 knockdown, which both increases snRNA levels and partially rescues some splicing defects.

Prevention of snRNA Decapping May Lead to Rescue of snRNP Function. There is ample evidence in the literature to suggest that the minor spliceosome is affected under conditions of low SMN (14, 53). Consistent with previous results, we observe that SMN KD leads to reduced levels of U1, U5, U11, U12, and U4atac snRNAs (Fig. 5*A*). A reduction in U11, U12, and U4atac snRNA levels also leads to splicing defects in transcripts that contain introns spliced via U12-dependent splicing (Fig. 6*A* and Fig. S5*A*). Further, knockdown of the decapping enzyme DCP2, but not the 5′-to-3′ exonuclease XRN1, leads to partial rescue of the splicing defects observed upon SMN KD (Fig. 6*A* and Fig. S5*A*). The competition between snRNP assembly and degradation suggests that limiting snRNA degradation pathways might be a possible therapeutic route to restoring the reduced snRNA levels seen in SMA models. Further altering this competition could be relevant in rescuing the function of snRNPs in splicing.

These results indicate that although XRN1 KD could stabilize snRNA levels (Fig. 6*C*), some (or all) of these snRNAs might be missing the 5′ cap structure, which leads to a nonfunctional pool of snRNAs unable to participate in splicing. On the other hand, knockdown of DCP2 protects the cap structure of some snRNAs,

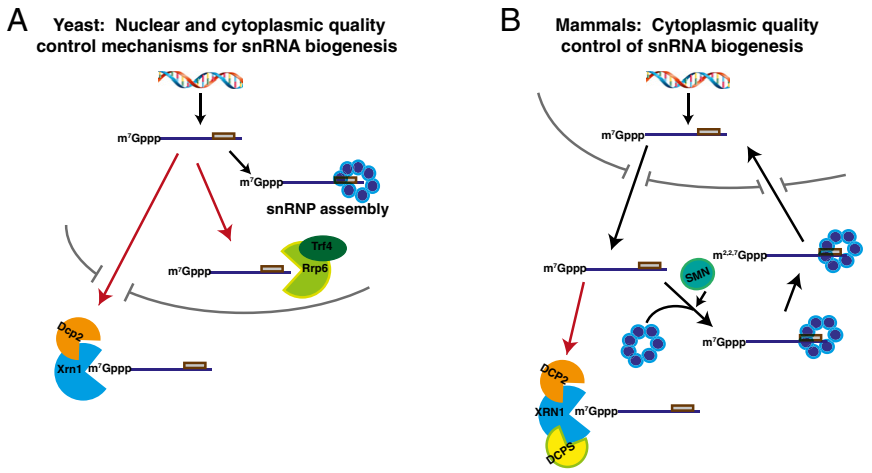

Fig. 7. Proposed model for snRNA quality control in yeast and mammals. (*A*) In yeast, snRNAs defective in snRNP assembly are degraded both in the nucleus by Rrp6p/Trf4p and in the cytoplasm by Dcp1p/Dcp2p-mediated decapping and Xrn1p-mediated decay. (*B*) In mammals, snRNAs exported to the cytoplasm for snRNP assembly are degraded under SMN-limiting conditions due to competition with quality control mechanisms. The model indicates one possible mode of DCPS's role in snRNA quality control, and other roles of DCPS are possible. Prevention of cytoplasmic 5′-3′ decay, either by RNAi in our experiment or through a drug inhibitor, could prevent snRNA degradation and increase the pool of available snRNAs in the cell.

making them inaccessible to XRN1-dependent digestion and able to participate in splicing. The cap structure is especially important because after Sm complex assembly, the m^7G cap on the snRNA is modified to the $m^{2,2,7}G$ trimethylated structure, which serves as a nuclear localization signal for further snRNP maturation and participation in splicing (8, 54). Therefore, prevention of snRNA decapping could be a relevant strategy to ameliorate snRNA reductions due to SMN defects, although it is still unresolved whether snRNA-level reductions underlie the pathology of SMA (18, 19).

Interestingly, one of the current drug candidates in clinical trials for SMA is a quinazoline derivative that inhibits DCPS and resembles a general m^7G cap structure (55–57). Whereas it was earlier believed that the DCPS inhibitor increases the levels of the SMN2 transcript in the cell (57), in at least one mouse model, treatment with the inhibitor has no effect on SMN protein levels in the organism (56). We suggest that this drug's efficacy in SMA mouse models may be due to its repression of the competing snRNA degradation pathway, thereby giving more time for snRNP assembly with limited SMN.

RNP Biogenesis Generally Competes with Quality Control. These results highlight a general principle wherein competition between RNP assembly pathways and degradation mechanisms has two consequences. First, such degradation systems function as a quality control mechanism to reduce the levels of defective RNAs (reviewed in refs. 1 and 2). Moreover, such degradation systems serve to amplify minor kinetic defects in RNP assembly, for example the reduction in snRNA levels under low levels of SMN, and potentially create a pathogenic condition. Thus, for mutations whose consequence is for RNP assembly per se, and not RNP function, we suggest that such RNP assembly mutations would be suppressed and pathogenesis avoided in the absence of competing RNA degradation systems. Note that such mutations could be either in RNAs, RNP components, or assembly machines.

RNP Assembly Diseases: An Emerging Class of Human Diseases. The competition between RNP assembly and RNA quality control mechanisms is a general phenomenon that appears to affect multiple human diseases (Table 1). For example, cartilage hair hypoplasia has been attributed to mutations in the RNA component of the RNase MRP holoenzyme (58), wherein disease-causing mutations reduce the levels and stability of MRP RNA (59, 60). Similarly in dyskeratosis congenita, mutations in either telomerase RNA or dyskerin can lead to reduced telomerase RNA levels (61–64). Moreover, the developmental disorder microcephalic osteodysplastic primordial dwarfism type I is caused by mutations in the gene coding for U4atac snRNA (65, 66), some of which reduce U4atac RNA levels possibly by affecting snRNP assembly (67). An important point is that for all of these disease conditions, we hypothesize that quality control pathways for RNA are reducing the concentrations of the relevant RNAs. This suggests that targeting such RNA decay pathways might be an effective therapeutic approach provided that the resulting RNP is still at least partially functional, which will be the case when the defect is in RNP assembly and not in a downstream function.

Table 1. Possible RNP assembly diseases

Disease	Gene	Phenotype	Effect on RNA levels
Spinal muscular atrophy	SMN1	Lower motor neuron loss; severe forms fatal in infancy	snRNA levels decrease (12, 14, 15)
Microcephalic osteodysplastic primordial dwarfism I	RNU4atac	Dwarfism associated with stunted growth	U4atac snRNA levels low (65–67)
Cartilage hair hypoplasia	RMRP	Dwarfism, abnormal growth and sparse hair, bone dysfunction	MRP RNA levels low (60)
Dyskeratosis congenita	DKC1/TERC/TINF2	Shortened telomeres; bone marrow failure; progressive leading to death	Telomerase RNA levels low (61, 63, 64)

A list of RNP assembly diseases as described in the literature. A common feature of these diseases is a mutation affecting the stability of the RNA component of the RNP, potentially leading to its faster degradation by specific quality control pathways.

Materials and Methods

Construction of U1 Sm Mutants in Yeast and Mammals. Yeast Gal-U1 plasmid was a kind gift from Michael Rosbash (Brandeis University, Waltham, MA). Human U1 plasmid was a kind gift from Samuel Gunderson (Rutgers University, Piscataway, NJ). The mutations were created by the QuikChange II Mutagenesis Kit (Agilent Technologies) using primers specific to the mutated U1 gene, and the mutated plasmid was verified by Sanger sequencing.

Yeast Strains and Plasmids. The following yeast strains were used for this study: *WT*-yRP840 or yRP2856, *edc3Δ*-yRP1745, *dcp1Δ*-yRP1200, *xrn1Δ*-yRP1199, *rrp6Δ*-yRP1377, *rai1Δ*-yRP2921, *ski2Δ*-yRP1192, *ski7Δ*-yRP1533, *trf4Δ*-yRP2922, *xrn1Δ rrp6Δ*-yRP2923, *dcp2-7 rrp6Δ*-yRP2924, *dcp2Δ*-yRP2859, *dcs1Δ*-yRP2876, and *dcs1Δ rrp6Δ*-yRP2929. Additional details of strains and plasmids are available in SI (Tables S2 and S3).

Northern Blotting from Yeast Cultures and Quantification. Cultures were grown in a 2% (vol/vol) galactose, 1% sucrose medium to OD ∼0.5 and pelleted for steady-state experiments. For decay rate measurements, cultures were grown to OD ∼0.5 in 2% (vol/vol) galactose, 1% sucrose medium, pelleted, and resuspended in 2% (vol/vol) dextrose medium. Time points were taken from the culture at the desired durations. RNA extraction was carried out using a phenol:chloroform extraction protocol (68). The RNA was separated on a 6% polyacrylamide denaturing gel at 300 V for 9 h, transferred to a Nytran membrane (GE Healthcare Biosciences), and probed with a radioactive oligonucleotide complementary to the Hel VII mutation on the RNA (oRP1710) (Table S4). The blot was then exposed to a PhosphorImager screen, and the signal was visualized on a Typhoon 9410 PhosphorImager (GE Healthcare). The bands were quantified using ImageQuant 5.2 software.

All quantification includes average ± SD for the indicated number of replicates. Significant differences were calculated using one-tailed unpaired Student's *t* test, with *P* values less than 0.05 denoted by an asterisk.

Mammalian Cell Culture. HeLa and NIH 3T3 cell lines purchased from ATCC were used for mammalian cell-culture experiments. The cells were grown in appropriate volume of 10% FBS in DMEM, supplemented with nonessential amino acids (Life Technologies), L-GlutaMAX, 1% penicillin/streptomycin, and sodium pyruvate. All cultures were grown in a 37-°C incubator with 5% CO_2 under normal humidity.

Plasmid Transfection in Mammalian Cells. Cells (12×10^4) were plated on a six-well plate in 10% FBS in DMEM lacking antibiotics. Three hundred nanograms of the appropriate plasmid was transfected per well using DharmaFECT 1 (Thermo Scientific) per the manufacturer's specifications. Cells were grown in Opti-MEM I reduced serum medium (Life Technologies) for 6 h, and then shifted to complete growth medium. Analysis was carried out 24 h post-transfection. For knockdown experiments, the cells were cotransfected with 300 ng of the U1-C4 plasmid along with 25 nM siRNA of choice, and analysis was performed after 24 h.

RNA Interference in Mammalian Cultures. For HeLa cells, 12×10^4 cells were plated in a six-well plate in 10% FBS in DMEM without antibiotics. For NIH 3T3 fibroblasts, 20×10^4 cells were plated in a six-well plate in 10% FBS in DMEM without antibiotics. Transfection was carried out using DharmaFECT 1 (Thermo Scientific) and Opti-MEM I reduced serum medium (Life Technologies) per the manufacturer's specifications. siRNAs targeting genes of interest were purchased (Qiagen) and 25 nM siRNA was used per well per knockdown. Cells were grown in Opti-MEM I, and then shifted to normal growth medium after 24 h. For double knockdowns, selected wells were transfected with the second siRNA (25 nM) 24 h after transfection with the SMN siRNA (25 nM for HeLa cells, 30 nM for 3T3 cells), whereas the other wells were mock transfected. Knockdown was allowed to go on for 3 d in total before analysis was performed.

Western Blotting from Mammalian Cells. Posttransfection, cells were washed with 1× Dulbecco's Phosphate Buffered Saline (Life Technologies) twice and harvested using passive lysis buffer. Approximately 10 μg of total protein was separated on 4–12% bis-Tris precast gels purchased from Life Technologies. The protein was transferred to a Protran membrane (Thermo Scientific) and blotted with the appropriate antibodies in 5% milk powder solution in 1XTBS with 0.5% Tween 20. The antibodies used were as follows: mouse anti-SMN (BD Biosciences), rabbit anti-DCP2 (Bethyl), rabbit anti-XRN1 (Bethyl), rabbit anti-EXOSC10 (Pierce), rabbit anti-DCPS (Pierce), rabbit anti-GAPDH (Cell Signaling), rabbit anti-NUDT16 (Proteintech), and rabbit anti–α-tubulin (Cell Signaling). Signal was visualized using SuperSignal West Dura Extended Duration Substrate (Pierce).

Northern Blotting from Mammalian Cells and Quantification. Posttransfection, cells were washed twice with 1× DPBS and harvested using TRIzol (Life Technologies). RNA was extracted using the TRIzol extraction protocol per the manufacturer's specifications, and separated on a 6% polyacrylamide denaturing gel at 300 V for 4.5 h. The RNA was transferred to a nylon membrane and probed with radioactive oligonucleotides specific to the transfected U1 plasmid (oRP1711) or to endogenous snRNAs (sequence information is available in Table S4). Signal was visualized on a Typhoon 9410 PhosphorImager.

All quantification includes average ± SD for the indicated number of replicates. Significant differences were calculated using one-way ANOVA for comparison of all groups and subsequently one-tailed unpaired Student's *t* test to calculate the significant differences ($*P < 0.05$).

RT-PCR and Splicing Assay from NIH 3T3 Cells. RNA was extracted as described above and treated with Turbo DNase (Invitrogen) to remove contamination. One microgram of total RNA was used for cDNA synthesis using an RNA to cDNA Ecodry Premix Kit (Clontech). Product (2.5%) was used for semi-quantitative PCR amplification using primers described previously (14). The PCR product was then resolved on a 1.5% agarose gel and visualized using GelRed staining on a FluorChem HD2 (ProteinSimple).

The mature:precursor transcript ratio was calculated by quantifying the intensity of the respective bands using ImageJ software (National Institutes of Health). Averages and SDs are shown for the indicated number of replicates.

ACKNOWLEDGMENTS. We thank Dr. Michael Rosbash (Brandeis University) for the generous gift of the yeast Gal-U1 plasmid, and Dr. Samuel Gunderson (Rutgers University) for the generous gift of the human U1 plasmid. We also thank all members of the R.P. laboratory for helpful discussions and suggestions. S.S. extends a special thanks to Dr. Robert Walters for his help with the mammalian cell-culture experiments, and to Anne Webb for her help with the illustrations used in this manuscript. This work was supported by a grant from the National Institutes of Health (to R.P.; R37GM45443) and by funds from the Howard Hughes Medical Institute.

1. Houseley J, Tollervey D (2009) The many pathways of RNA degradation. *Cell* 136(4):763–776.
2. Doma MK, Parker R (2007) RNA quality control in eukaryotes. *Cell* 131(4):660–668.
3. Jones MH, Guthrie C (1990) Unexpected flexibility in an evolutionarily conserved protein-RNA interaction: Genetic analysis of the Sm complex binding site. *EMBO J* 9(8):2555–2561.
4. Seto AG, Zaug AJ, Sobel SG, Wolin SL, Cech TR (1999) *Saccharomyces cerevisiae* telomerase is an Sm small nuclear ribonucleoprotein particle. *Nature* 401(6749):177–180.
5. Hamm J, Dathan NA, Scherly D, Mattaj IW (1990) Multiple domains of U1 snRNA, including U1 specific protein binding sites, are required for splicing. *EMBO J* 9(4):1237–1244.
6. Lorson CL, Rindt H, Shababi M (2010) Spinal muscular atrophy: Mechanisms and therapeutic strategies. *Hum Mol Genet* 19(R1):R111–R118.
7. Lefebvre S, et al. (1995) Identification and characterization of a spinal muscular atrophy-determining gene. *Cell* 80(1):155–165.
8. Neuenkirchen N, Chari A, Fischer U (2008) Deciphering the assembly pathway of Sm-class U snRNPs. *FEBS Lett* 582(14):1997–2003.
9. Battle DJ, et al. (2006) The SMN complex: An assembly machine for RNPs. *Cold Spring Harb Symp Quant Biol* 71:313–320.
10. Fischer U, Englbrecht C, Chari A (2011) Biogenesis of spliceosomal small nuclear ribonucleoproteins. *Wiley Interdiscip Rev RNA* 2(5):718–731.
11. Wan L, et al. (2005) The survival of motor neurons protein determines the capacity for snRNP assembly: Biochemical deficiency in spinal muscular atrophy. *Mol Cell Biol* 25(13):5543–5551.
12. Zhang Z, et al. (2008) SMN deficiency causes tissue-specific perturbations in the repertoire of snRNAs and widespread defects in splicing. *Cell* 133(4):585–600.
13. Workman E, et al. (2009) A SMN missense mutation complements SMN2 restoring snRNPs and rescuing SMA mice. *Hum Mol Genet* 18(12):2215–2229.
14. Lotti F, et al. (2012) An SMN-dependent U12 splicing event essential for motor circuit function. *Cell* 151(2):440–454.
15. Gabanella F, et al. (2007) Ribonucleoprotein assembly defects correlate with spinal muscular atrophy severity and preferentially affect a subset of spliceosomal snRNPs. *PLoS ONE* 2(9):e921.
16. Zhang Z, et al. (2013) Dysregulation of synaptogenesis genes antecedes motor neuron pathology in spinal muscular atrophy. *Proc Natl Acad Sci USA* 110(48):19348–19353.
17. Burghes AHM, Beattie CE (2009) Spinal muscular atrophy: Why do low levels of survival motor neuron protein make motor neurons sick? *Nat Rev Neurosci* 10(8):597–609.
18. Bäumer D, et al. (2009) Alternative splicing events are a late feature of pathology in a mouse model of spinal muscular atrophy. *PLoS Genet* 5(12):e1000773.

19. Praveen K, Wen Y, Matera AG (2012) A *Drosophila* model of spinal muscular atrophy uncouples snRNP biogenesis functions of survival motor neuron from locomotion and viability defects. *Cell Reports* 1(6):624–631.
20. Garcia EL, Lu Z, Meers MP, Praveen K, Matera AG (2013) Developmental arrest of *Drosophila* survival motor neuron (Smn) mutants accounts for differences in expression of minor intron-containing genes. *RNA* 19(11):1510–1516.
21. Winkler C, et al. (2005) Reduced U snRNP assembly causes motor axon degeneration in an animal model for spinal muscular atrophy. *Genes Dev* 19(19):2320–2330.
22. See K, et al. (2014) SMN deficiency alters Nrxn2 expression and splicing in zebrafish and mouse models of spinal muscular atrophy. *Hum Mol Genet* 23(7):1754–1770.
23. Liao XL, Kretzner L, Seraphin B, Rosbash M (1990) Universally conserved and yeast-specific U1 snRNA sequences are important but not essential for U1 snRNP function. *Genes Dev* 4(10):1766–1774.
24. Seipelt RL, Zheng B, Asuru A, Rymond BC (1999) U1 snRNA is cleaved by RNase III and processed through an Sm site-dependent pathway. *Nucleic Acids Res* 27(2):587–595.
25. Parker R (2012) RNA degradation in *Saccharomyces cerevisae*. *Genetics* 191(3): 671–702.
26. Schmid M, Jensen TH (2008) The exosome: A multipurpose RNA-decay machine. *Trends Biochem Sci* 33(10):501–510.
27. Wyers F, et al. (2005) Cryptic pol II transcripts are degraded by a nuclear quality control pathway involving a new poly(A) polymerase. *Cell* 121(5):725–737.
28. Kadaba S, et al. (2004) Nuclear surveillance and degradation of hypomodified initiator tRNAMet in *S. cerevisiae*. *Genes Dev* 18(11):1227–1240.
29. Vanácová S, et al. (2005) A new yeast poly(A) polymerase complex involved in RNA quality control. *PLoS Biol* 3(6):e189.
30. LaCava J, et al. (2005) RNA degradation by the exosome is promoted by a nuclear polyadenylation complex. *Cell* 121(5):713–724.
31. Liu H, Rodgers ND, Jiao X, Kiledjian M (2002) The scavenger mRNA decapping enzyme DcpS is a member of the HIT family of pyrophosphatases. *EMBO J* 21(17):4699–4708.
32. Chang JH, et al. (2012) Dxo1 is a new type of eukaryotic enzyme with both decapping and 5′-3′ exoribonuclease activity. *Nat Struct Mol Biol* 19(10):1011–1017.
33. Jiao X, et al. (2010) Identification of a quality-control mechanism for mRNA 5′-end capping. *Nature* 467(7315):608–611.
34. Haimovich G, et al. (2013) Gene expression is circular: Factors for mRNA degradation also foster mRNA synthesis. *Cell* 153(5):1000–1011.
35. Dunckley T, Tucker M, Parker R (2001) Two related proteins, Edc1p and Edc2p, stimulate mRNA decapping in *Saccharomyces cerevisiae*. *Genetics* 157(1):27–37.
36. Olson BL, Siliciano PG (2003) A diverse set of nuclear RNAs transfer between nuclei of yeast heterokaryons. *Yeast* 20(10):893–903.
37. Beckley SA, et al. (2001) Reduction of target gene expression by a modified U1 snRNA. *Mol Cell Biol* 21(8):2815–2825.
38. Li Y, Kiledjian M (2010) Regulation of mRNA decapping. *Wiley Interdiscip Rev RNA* 1(2):253–265.
39. Song M-G, Li Y, Kiledjian M (2010) Multiple mRNA decapping enzymes in mammalian cells. *Mol Cell* 40(3):423–432.
40. Li Y, Song M, Kiledjian M (2011) Differential utilization of decapping enzymes in mammalian mRNA decay pathways. *RNA* 17(3):419–428.
41. Scarsdale JN, Peculis BA, Wright HT (2006) Crystal structures of U8 snoRNA decapping Nudix hydrolase, X29, and its metal and cap complexes. *Structure* 14(2):331–343.
42. Pellizzoni L, Yong J, Dreyfuss G (2002) Essential role for the SMN complex in the specificity of snRNP assembly. *Science* 298(5599):1775–1779.
43. Meister G, Bühler D, Pillai R, Lottspeich F, Fischer U (2001) A multiprotein complex mediates the ATP-dependent assembly of spliceosomal U snRNPs. *Nat Cell Biol* 3(11): 945–949.
44. Shpargel KB, Matera AG (2005) Gemin proteins are required for efficient assembly of Sm-class ribonucleoproteins. *Proc Natl Acad Sci USA* 102(48):17372–17377.
45. Ishikawa H, et al. (2014) Identification of truncated forms of U1 snRNA reveals a novel RNA degradation pathway during snRNP biogenesis. *Nucleic Acids Res* 42(4):2708–2724.
46. Sheth U, Parker R (2003) Decapping and decay of messenger RNA occur in cytoplasmic processing bodies. *Science* 300(5620):805–808.
47. Parker R, Sheth U (2007) P bodies and the control of mRNA translation and degradation. *Mol Cell* 25(5):635–646.
48. Song M-G, Bail S, Kiledjian M (2013) Multiple Nudix family proteins possess mRNA decapping activity. *RNA* 19(3):390–399.
49. Li Y, Song M-G, Kiledjian M (2008) Transcript-specific decapping and regulated stability by the human Dcp2 decapping protein. *Mol Cell Biol* 28(3):939–948.
50. Liu H, Kiledjian M (2005) Scavenger decapping activity facilitates 5′ to 3′ mRNA decay. *Mol Cell Biol* 25(22):9764–9772.
51. Sinturel F, Bréchemier-Baey D, Kiledjian M, Condon C, Bénard L (2012) Activation of 5′-3′ exoribonuclease Xrn1 by cofactor Dcs1 is essential for mitochondrial function in yeast. *Proc Natl Acad Sci USA* 109(21):8264–8269.
52. Bossé GD, et al. (2013) The decapping scavenger enzyme DCS-1 controls microRNA levels in *Caenorhabditis elegans*. *Mol Cell* 50(2):281–287.
53. Boulisfane N, et al. (2011) Impaired minor tri-snRNP assembly generates differential splicing defects of U12-type introns in lymphoblasts derived from a type I SMA patient. *Hum Mol Genet* 20(4):641–648.
54. Mattaj IW (1986) Cap trimethylation of U snRNA is cytoplasmic and dependent on U snRNP protein binding. *Cell* 46(6):905–911.
55. Gogliotti RG, et al. (2013) The DcpS inhibitor RG3039 improves survival, function and motor unit pathologies in two SMA mouse models. *Hum Mol Genet* 22(20): 4084–4101.
56. Van Meerbeke JP, et al. (2013) The DcpS inhibitor RG3039 improves motor function in SMA mice. *Hum Mol Genet* 22(20):4074–4083.
57. Singh J, et al. (2008) DcpS as a therapeutic target for spinal muscular atrophy. *ACS Chem Biol* 3(11):711–722.
58. Ridanpää M, et al. (2001) Mutations in the RNA component of RNase MRP cause a pleiotropic human disease, cartilage-hair hypoplasia. *Cell* 104(2):195–203.
59. Nakashima E, et al. (2007) Cartilage hair hypoplasia mutations that lead to RMRP promoter inefficiency or RNA transcript instability. *Am J Med Genet A* 143A(22): 2675–2681.
60. Hermanns P, et al. (2006) RMRP mutations in cartilage-hair hypoplasia. *Am J Med Genet A* 140(19):2121–2130.
61. Brault ME, Lauzon C, Autexier C (2013) Dyskeratosis congenita mutations in dyskerin SUMOylation consensus sites lead to impaired telomerase RNA accumulation and telomere defects. *Hum Mol Genet* 22(17):3498–3507.
62. Mason PJ, Bessler M (2011) The genetics of dyskeratosis congenita. *Cancer Genet* 204(12):635–645.
63. Vulliamy T, et al. (2001) The RNA component of telomerase is mutated in autosomal dominant dyskeratosis congenita. *Nature* 413(6854):432–435.
64. Wong JMY, Collins K (2006) Telomerase RNA level limits telomere maintenance in X-linked dyskeratosis congenita. *Genes Dev* 20(20):2848–2858.
65. He H, et al. (2011) Mutations in U4atac snRNA, a component of the minor spliceosome, in the developmental disorder MOPD I. *Science* 332(6026):238–240.
66. Edery P, et al. (2011) Association of TALS developmental disorder with defect in minor splicing component U4atac snRNA. *Science* 332(6026):240–243.
67. Jafarifar F, Dietrich RC, Hiznay JM, Padgett RA (2014) Biochemical defects in minor spliceosome function in the developmental disorder MOPD I. *RNA* 20(7):1078–1089.
68. Muhlrad D, Parker R (1999) Aberrant mRNAs with extended 3′ UTRs are substrates for rapid degradation by mRNA surveillance. *RNA* 5(10):1299–1307.